

A Study of Ultra-Luminous X-ray Sources from the Chandra Archive of Galaxies

Douglas A. Swartz¹, Kajal K. Ghosh¹, Allyn F. Tennant²

Presented to the American Astronomical Society Meeting 201, 54.13

ABSTRACT

The more than 80 nearby galaxies imaged with the Chandra Advanced CCD Imaging Spectrometer have been analyzed in a search for Ultra-Luminous X-ray (ULX) sources. The sample of galaxies span the range of Hubble morphological types and include galaxies of various mass, gas content, and dynamical state. X-ray characteristics of the resulting ensemble of ULX candidates are reported and correlations with properties of the host galaxies are presented.

Support for this research was provided in part by NASA/Chandra grant AR2-3008X to D.A.S.

1. Introduction

Among the most intriguing objects in the X-ray sky are the non-nuclear Ultra-Luminous X-ray (ULX) sources in nearby galaxies. This name describes those sources considerably more luminous than expected for a spherically-accreting object of typical neutron star mass. Here, we define ULX sources to be those with apparent (i.e., assumed isotropically emitting) intrinsic luminosities in excess of 10^{39} erg/s in the 0.5-8.0 keV bandpass.

Through the first 2 years or so of operation, the Chandra X-ray Observatory (CXO) has imaged enough nearby galaxies using the ACIS CCD Imaging Spectrometer to undertake a systematic and uniform analysis of their ULX population. Ultimately, we wish to know the full pedigree of these extreme objects: what are their origins and history; why and how do they differ from their more-common low-luminosity cousins; what does the population of ULX sources reveal about the nature of galaxy formation and evolution; and what influence do ULX sources have on their local environments? Here, we report principally the correlations between ULXs and global properties of their host galaxies.

¹Universities Space Research Association, NASA Marshall Space Flight Center, SD50, Huntsville, AL, USA

²Space Science Department, NASA Marshall Space Flight Center, SD50, Huntsville, AL, USA

2. X-Ray Data Reduction Methods

Based on integration time and the best distance estimate available, we selected all those galaxies for which ~ 100 source counts are expected from a ULX. In integration time units of ks and distances in Mpc, this corresponds to observations with $t/D \gtrsim 0.12$. To date, 85 galaxies in the CXC public archive meet this selection criterion.

For all candidate galaxy ACIS images, the following steps were taken:

- All events within the D_{25} isophote were extracted from Level 2 event files.
- X-ray sources (to ~ 3.5 S/N) were located using standard methods.
- Source and local background spectra in the 0.5 – 8.0 keV energy range were extracted.
- Source count rates were determined and the source list ordered by decreasing count rate.
- The (binned) time series for each source and for the entire image field were constructed (the latter to help identify and eliminate high noise level intervals).
- Beginning with highest count-rate sources, simple models were fit to the spectra to establish spectral shapes and source luminosities. This process was extended to sources well below the 10^{39} erg/s ULX lower limit to ensure completeness of the sample for each galaxy. Sources within $5''$ of the host galaxy center were omitted from consideration.
- Source positions were overlaid on optical images (usually DSS) to crudely map source locations to morphological features of host galaxies and to help eliminate obvious foreground objects. Similarly, ULX candidate source positions were queried using the NASA/IPAC Extragalactic Database to help eliminate known background QSOs.

3. The Sample of Galaxies

The CXO sample of galaxies is compared to the Tully catalogue of 2368 nearby galaxies in the two figures shown above. The CXO sample is composed of mostly nearby galaxies (Figure 1, left, note the large step at the Virgo cluster distance), with 1/2 the sample within 10 Mpc, and they are typically brighter in Blue luminosity (Figure 1, right). Throughout this work, the blue luminosity is used as a proxy for galaxy mass. Although blue light is more sensitive to the properties of the stellar population of the host galaxy than is visible light, the B-V colors of the CXO sample all fall within the range of 0.5 to 1.0 magnitudes and so B is a good measure of mass.

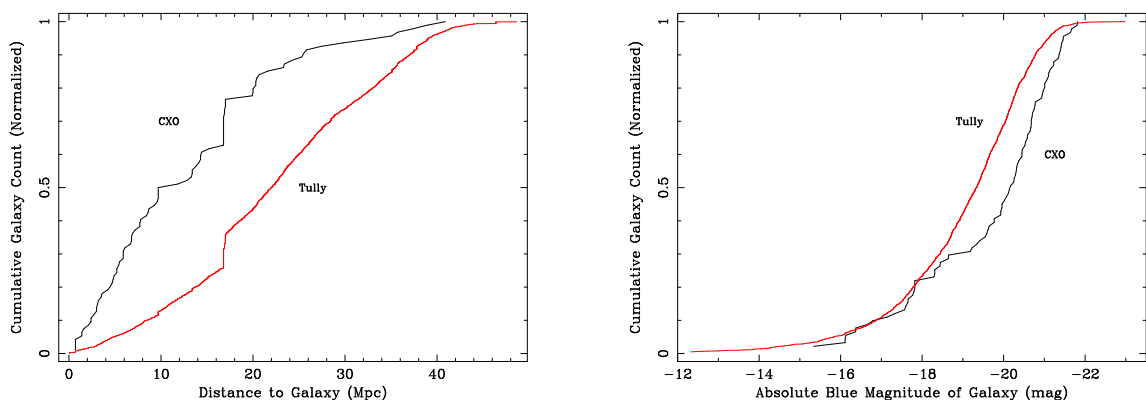


Fig. 1.— Cumulative distributions of the *Chandra* sample of galaxies compared to the Tully (1988) catalogue over distance (*left*) and blue luminosity (*right*).

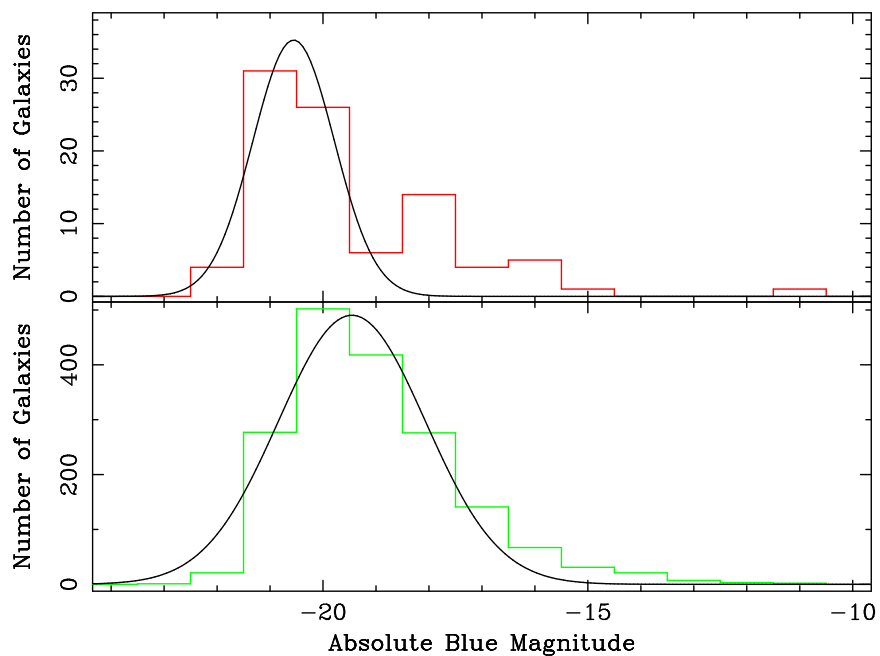


Fig. 2.— Distribution of blue luminosities of the *Chandra* sample (*top*) and Tully catalogue of galaxies.

Another means of displaying the dependence of the two samples on blue luminosity is shown in Figure 2. The mean absolute blue magnitude of the CXO sample is -20.6 or slightly brighter than that of the Tully catalogue at -19.4 .

The CXO sample of galaxies spans the entire range of Hubble morphological types (Figure 3). There are 32 elliptical and lenticular galaxies and 50 spiral and irregular galaxies in the sample.

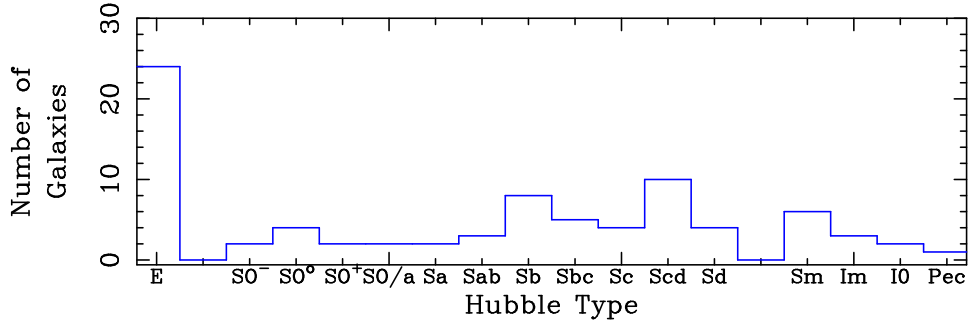


Fig. 3.— Distribution of Hubble morphological types among the *Chandra* sample of galaxies.

The distribution of the CXO sample of galaxies in blue and far-infrared (FIR) luminosity space is shown in Figure 4. The ellipticals are clustered near the upper left indicative of a relatively high mass per unit star-formation-rate (SFR) whereas the spiral galaxies generally span from lower-left to upper right in this plot going generally from small, late-type galaxies toward more massive early-type spirals. Note the several exceptions such as the starburst galaxy M82 ($L_{\text{FIR}} = 10^{44}$, $L_{\text{B}} = 2 \times 10^{42}$).

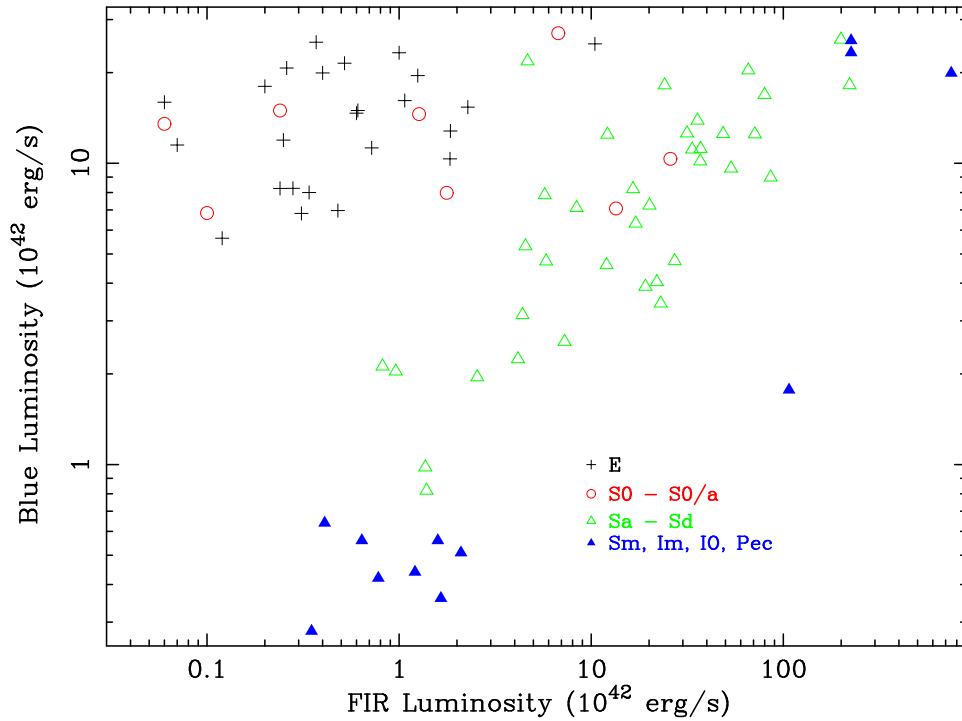


Fig. 4.— Distribution of the *Chandra* sample of galaxies in B and FIR luminosity.

4. Correlations with Galaxy Properties

We have searched for correlations between the number and luminosities of ULX sources with numerous galaxy properties. Examples are shown in Figures 5 and 6. The distribution of X-ray luminosities of individual ULXs against the host galaxy’s FIR luminosity is shown above and against the B luminosity is shown below. There is a distinct separation between elliptical and spiral galaxies in FIR luminosity but that simply reflects the sample (see Figure 4). There is also a trend toward brighter ULXs in the spiral galaxies. However, there is also more ULX candidates in those galaxies and this trend may simply be a statistical fluctuation. Similarly, in blue light, there are more and brighter ULX candidates per galaxy in more massive (higher B luminosity) galaxies. One expects to find more ULXs in more massive galaxies and perhaps, again, the trend toward more luminous ULXs is simply a statistical fluctuation.

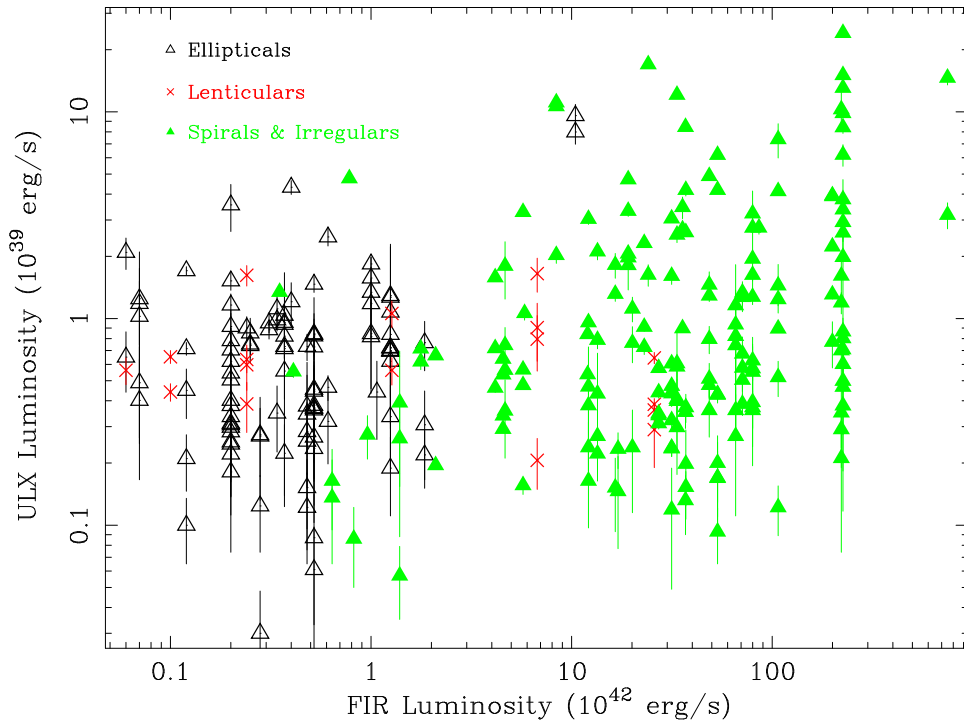


Fig. 5.— Distribution of the ULX X-ray luminosities with host galaxy FIR luminosity.

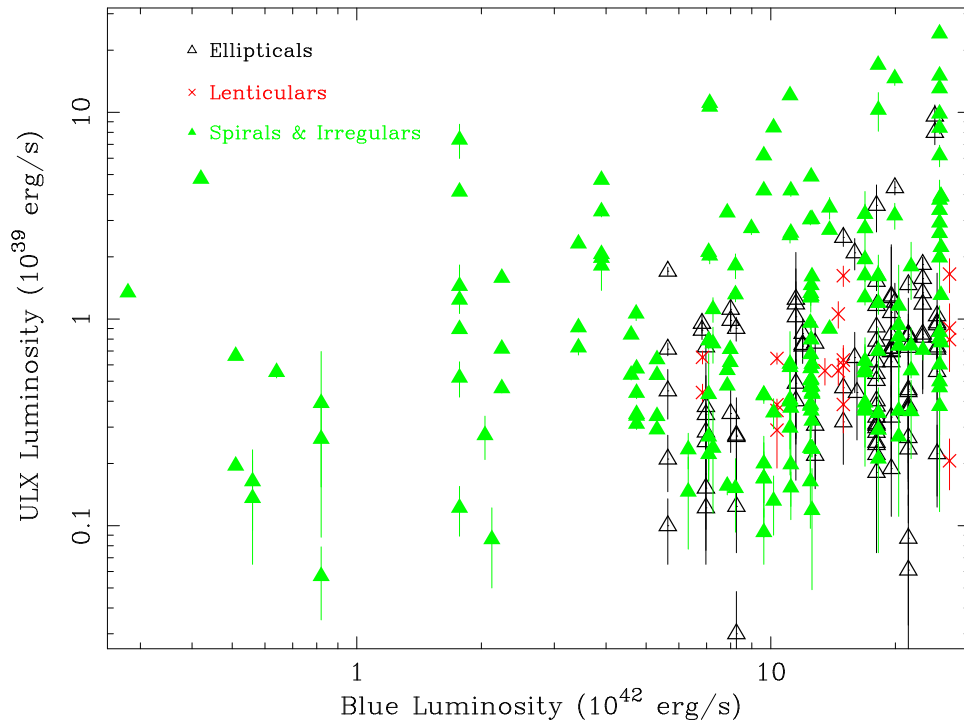


Fig. 6.— Distribution of the ULX X-ray luminosities with host galaxy B luminosity.

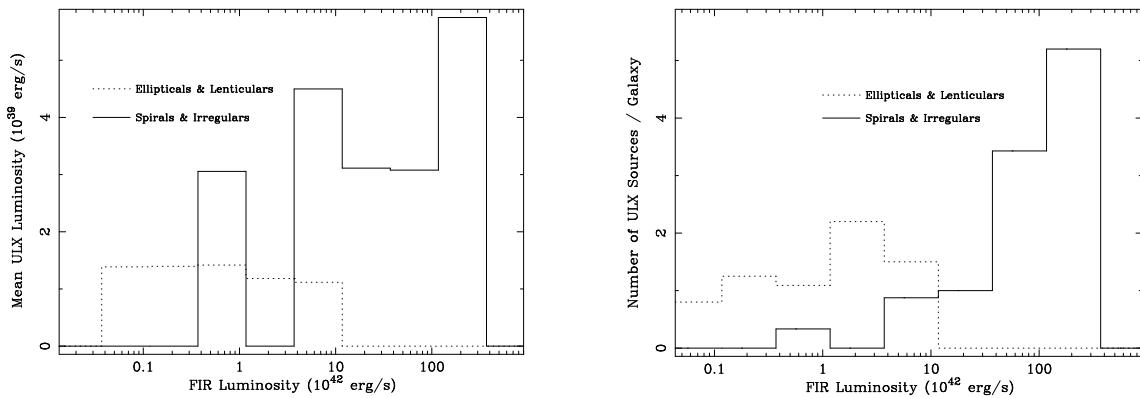


Fig. 7.— Mean ULX luminosity (*left*) and the number of ULX candidates per galaxy (*right*) against the FIR luminosity of the host galaxies.

The possible correlation with FIR luminosity is shown in a different way in Figure 7. Here, only the ULX sources with $L_X > 10^{39}$ erg/s are displayed. The figure at left shows that the brightest ULXs are indeed in the brightest FIR galaxies (although the distribution about the mean is broad, see Figure 6). The mean X-ray luminosity of ULXs in ellipticals is less than that in the spiral galaxies. At right we show that the number of ULXs per unit galaxy is strongly correlated with FIR luminosity.

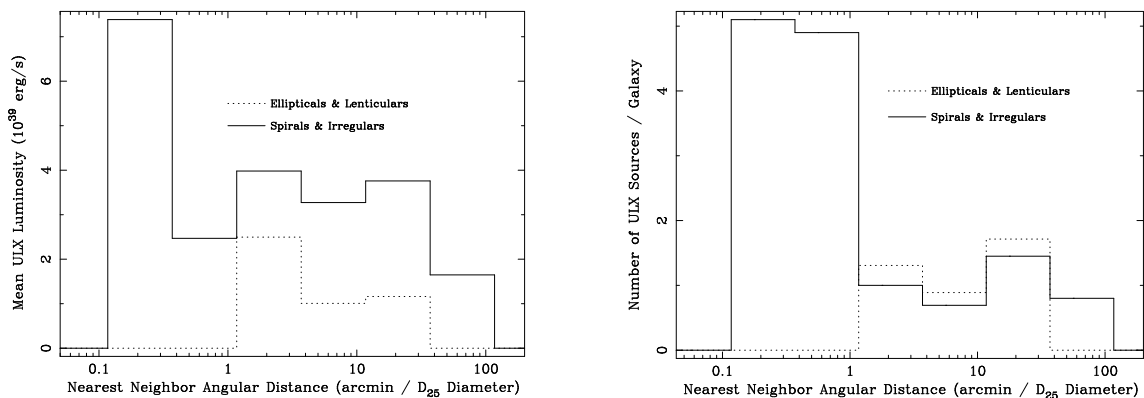


Fig. 8.— Mean ULX luminosity (*left*) and the number of ULX candidates per galaxy (*right*) against the distance to the nearest-neighbor of the host galaxies.

In Figure 8 we show the only other strong correlation we have found between the number and luminosities of ULX sources with galaxy properties, namely, the distance to the host galaxy’s nearest neighbor (measured in units of the D_{25} isophotal diameter). Those with separations <1 are in the process of merging. They show much more activity (and high FIR luminosity, typically) and tend to have many ULXs. Ellipticals and spirals with more distant neighbors have much fewer ULXs and they are not as luminous although those in spirals are still more luminous than those in ellipticals.

5. ULX X-Ray Spectral Properties

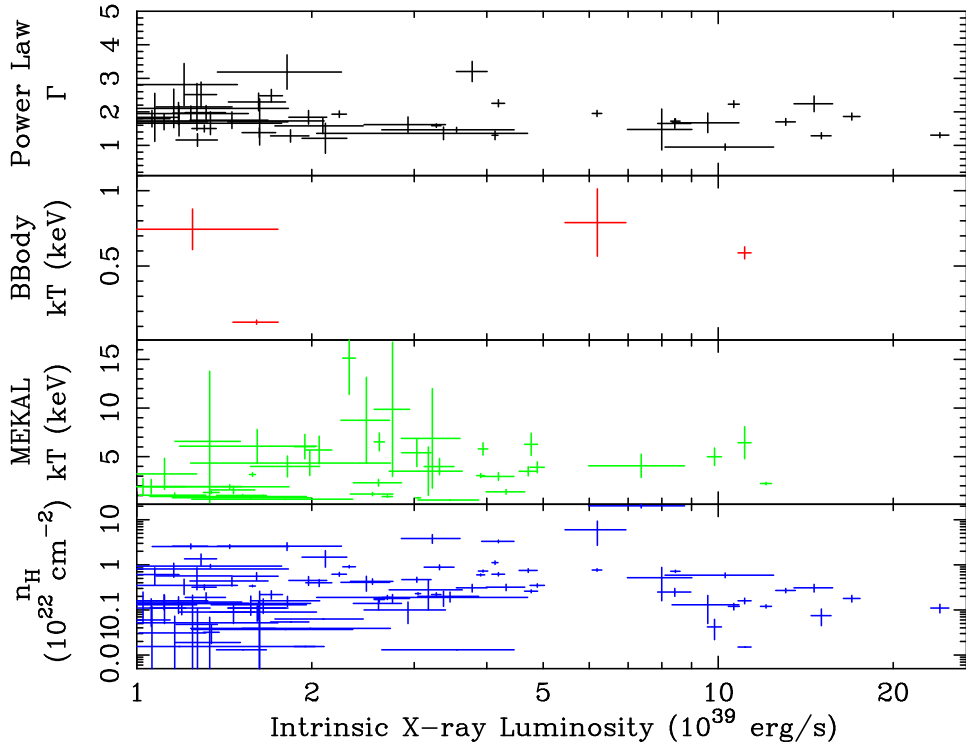


Fig. 9.— Distribution of the ULX X-ray spectral parameters.

In figure 9 is shown the distribution of the basic spectral parameters with the ULX source luminosities. Three simple models were used to characterize the 0.5 – 8.0 keV spectra of the ULX candidates. Statistically, about 50% were best-fit using an absorbed power law (mean spectral index for the group is 1.67) and about 50% are absorbed thermal emission spectra (mean temperature 2.9 keV). Only 5 or about 4% were best represented by an absorbed blackbody spectrum. Of course, many of the higher count sources will require more complex spectral models. This is work in progress. So far, no obvious correlation has been found between spectral properties and ULX luminosity nor with galaxy properties.

6. X-ray Luminosity Distributions

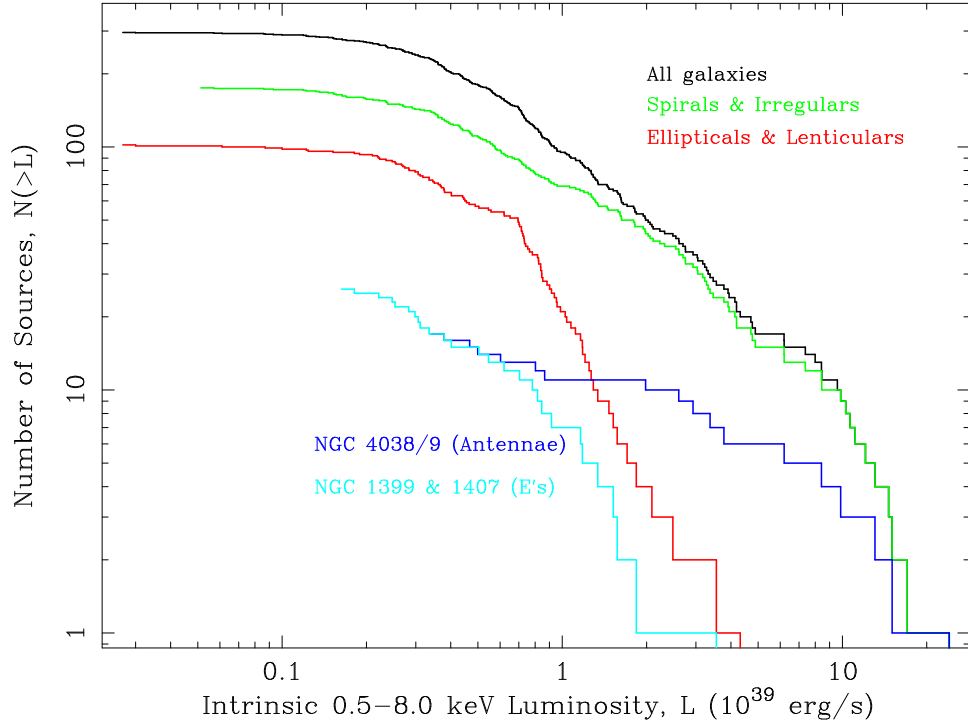


Fig. 10.— LogN-logS distributions for the sample of galaxies.

The luminosity functions of the entire CXO sample of ULX candidates is shown in Figure 10 along with the luminosity functions of the spirals and ellipticals. Also shown are a few of the galaxies with particularly high numbers of ULXs per galaxy. The horizontal scale has been extended to well below the ULX lower limit of 10^{39} erg/s to clearly show the incompleteness at low luminosities that results from our focus on the brightest objects. There are several features of interest. Clearly, the highest ULX luminosities in the spiral galaxies are much higher than those of the ellipticals and spirals dominate the total luminosity function throughout the entire range $L_X > 10^{39}$. (However, only $\sim 3/8$ of the galaxies are ellipticals and lenticulars, a factor that has not been accounted for here.) At the very highest end, the spirals are dominated by the single galaxy pair NGC 4038/9, with about 40% of the ULXs brighter than 5×10^{39} erg/s within that one system. The ellipticals exhibit a very different luminosity function. The slope of the elliptical galaxy luminosity function above 0.7×10^{39} erg/s is -2.3 compared to -0.9 for spirals in the range $(0.7 - 10) \times 10^{39}$ and to -1.0 for the entire sample on that range. Above 10^{40} erg/s, there is a steep decline or cutoff in the luminosity function of the sample. There is also a distinct change in slope in the luminosity function of the elliptical galaxies at 0.7×10^{39} erg/s. This is a real feature as opposed to the gradual flattening at low luminosities due to incompleteness (occurring in most of the

curves at around $(2 - 4) \times 10^{38}$ erg/s). Because of this incompleteness, it is not possible to distinguish any change in slope at 2×10^{38} , the Eddington limit for typical neutron star accretors.

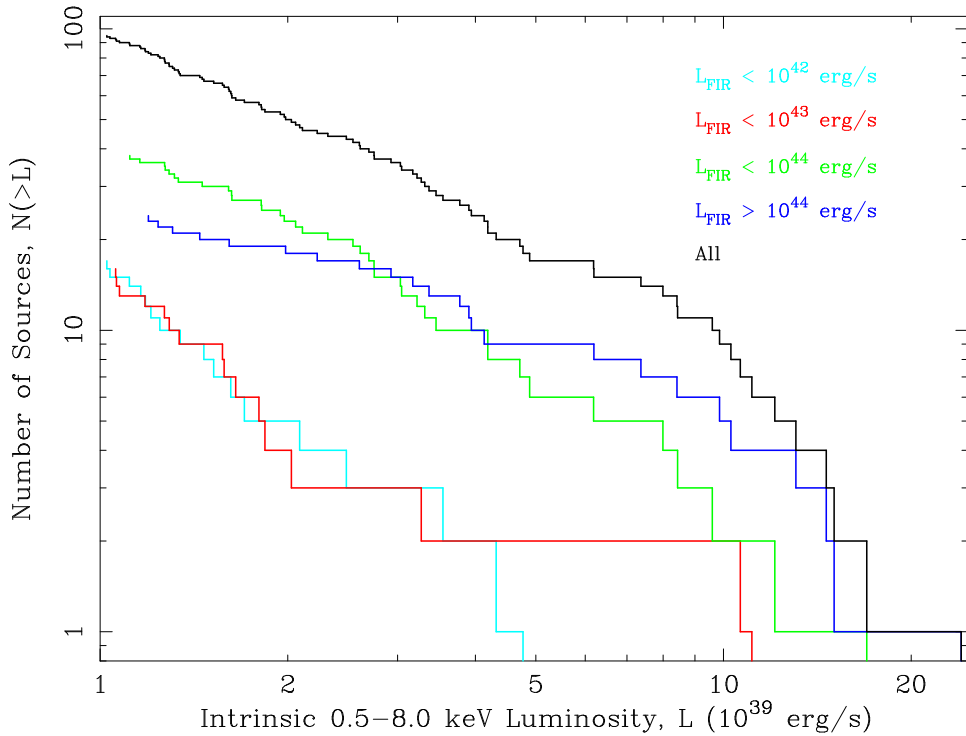


Fig. 11.— LogN-logS distributions for subsamples of the galaxies with different FIR luminosities.

The correlation of ULX X-ray luminosity with host galaxy FIR luminosity discussed previously is evident in the luminosity functions shown in Figure 11. Here, the CXO sample has been partitioned into FIR luminosity ranges. With the exception of 2 very bright sources in the $L_{\text{FIR}} = 10^{42}$ to 10^{43} erg/s range, there is a definite trend with the brightest ULXs occurring in the FIR-brightest hosts. (The 2 “exceptions” are both located in a galaxy with $L_{\text{FIR}} = 8.4 \times 10^{42}$, the brightest in the group and just below the upper limit of the range.)

7. Summary and Future Work

We have analyzed a sample of 85 galaxies available in the Chandra archive of ACIS images. About 120 ULX candidates have been identified and their spectral properties determined. Few correlations have been found so far between the number and luminosities of the ULX candidates and properties of the host galaxy population. Two correlations described

here are with the galaxy’s FIR luminosity and with the galaxy’s interacting or merging status as measured by the distance to its nearest neighbor.

Future research will include:

- Further searches for correlations with other galaxy properties including the distributions of sources within the galaxy, correlations with spiral arms, bulges, bars, globular clusters, etc., and AGN activity.
- Refined modeling of the observed X-ray spectra, particularly of the highest count-rate sources where this is justified statistically.
- Source position refinement by registering to accurately-known positions of optical objects in the field, although Chandra positions are typically known to ~ 0.6 arcsecs.
- Extension to other wavelengths, particularly using archival HST and radio data.
- Examination of sample biases and completeness.